
Using input warping to improve the Bayesian optimisation of a complex epidemiological model of the sharka virus

Victor Picheny · Coralie Picard · Gaël Thébaud

Received: date / Accepted: date

Abstract Optimizing black-box numerical models remains a challenge in many research fields. In this work, we focus on a Bayesian optimization approach, accounting for local invariances of the model with respect to its input variables. More precisely, we incorporate the prior knowledge that the model is insensitive to variations of some of its input variables when other input variables take a particular value. To this end, we propose a new warping technique applied to the parameter space that encode the invariances. This approach is tested on a simulation model of sharka disease spread and management that exhibits several invariances. We analyze the contribution of the warping on the Bayesian optimization of sharka control options. We show that the warping step significantly improves the rate of convergence of the BO algorithm.

Keywords Bayesian optimisation, warping, spatio temporal model, sharka

1 Introduction

Mathematical models are increasingly used in many research fields to understand and optimize a process. For instance, they are useful in epidemiology to predict epidemics and to propose efficient control options [4, 5, 18, 33, 1, 14, 34, 9]. However, these epidemiological studies are mostly focused on improving one control option which generally depends on only one or two parameters in their model, although various control actions are usually applied simultaneously to manage an epidemic. All these actions could be jointly optimized but taking into account numerous management

V. Picheny
MIAT, Université de Toulouse, INRA, Castanet-Tolosan, France
Tel.: +33561285551
E-mail: victor.picheny@inra.fr

C. Picard
BGPI, Montpellier SupAgro, INRA, Univ. Montpellier, Cirad, TA A-54/K, 34398, Montpellier

G. Thébaud
to do

parameters in an optimization problem can be difficult, especially when the management efficiency depends on the interaction between these parameters.

In this study, we analyse a simulation model of sharka disease spread and management. This disease, caused by a virus transmitted by aphids, is one of the most damaging diseases of stone fruit trees belonging to the genus *Prunus* (e.g. peach, apricot and plum) [3, 25]. Our model includes epidemiological parameters which vary between simulations, and various landscapes on which the virus can spread, which means that this model is stochastic. In addition, management parameters allow to simulate orchard surveillance. Here, we aim to optimize these management parameters using an efficient optimization algorithm.

Within the wide range of potential approaches to solve such optimization problems, black-box optimization methods have proven to be popular in this context [28], in particular because they are in essence non-intrusive: they only require pointwise evaluations of the model at hand (output value for a given set of inputs), as opposed to knowing the underlying mechanisms of the model, structural information, derivatives, etc. This greatly facilitates implementation and avoids developing tailored algorithms. In this work, we focus more particularly on the so-called *Bayesian optimization* (BO) approaches [17, 30], which are well-suited to tackle stochastic and expensive models.

In some cases, the user possesses relevant information regarding his model that could facilitate the optimization task. Accounting for this information within a black-box optimization framework (or rather: *grey box*) may be a challenging task as it is, in essence, unnatural. In this work, we focus on a particular type of information, which we refer to as *local invariance*: for some values of a subset of parameters, it is known that the model is insensitive to another subset of parameters. As an illustration, take a function y that depends on two discs, parameterized by $r_1 \in [0, r_{\max}]$ (radius of the first disc) and $r_2 \in [0, r_{\max}]$ (radius of the second disc) with $r_1 > r_2$. An action A_1 is conveyed on the first disc and another action A_2 on the second. Setting $r_1 = 0$, we have $r_2 = 0$, thus for any value of A_2 , y is not impacted. Taking into account such invariances would avoid wasting computational resources exploring those regions. Moreover, it would avoid the problem of having local *plateaus* of the optimization landscape, that are likely to slow down the optimization process or even prevent convergence to an optimum.

Intuitively, one may want to rework the definition of the parameters to optimize over in order to remove the invariances. However (as we show in 2), such a reformulation is not always possible. Here, we propose to keep the optimisation problem unchanged, and convey the invariance information to the BO algorithm directly, by applying a *warping* [31, 32] to the parameter space. In essence, it amounts to applying a specific deformation of the parameter space that reflects the invariance.

The remainder of this paper is structured as follows. Section 2 describes the sharka model and its invariances. Section 3 presents the basics of Bayesian optimization and Section 4 our warping strategy. Finally, section 5 analyses the efficiency of the warping on the sharka model.

2 Model description and problem set-up

The simulation model that we analyze in this work is a stochastic, spatially explicit, SEIR (susceptible-exposed-infectious-removed) model that simulates sharka spread and management actions [including surveillance, removals and replantations 22, 26, 27].

This model is orchard-based, with a discrete time step of one week. It allows to perform simulations on landscapes composed of uncultivated areas and patches on which peach trees are grown. The patches can be more or less aggregated in the landscape however, we only use in this work the 30 landscapes with a high level of patch aggregation as described by Picard et al. [19]. During the simulation, the trees in the patches are characterized by different states. When the simulation begins, they are not infected: they are in the “susceptible” state. Then, the virus is introduced the first year of the simulation in one of the patches and spreads through orchards (new introductions can also occur during the entire simulation on all patches). The virus causes changes in tree status: from “susceptible”, they become “exposed” (infected but not yet infectious or symptomatic), “infectious hidden” (after the end of the latent period), “infectious detected” (when specific symptoms are detected on the tree during a survey), and “removed” (when the tree is removed from the patch). The model output is an economic criterion, the net present value (NPV), which accounts for the benefit generated by the cultivation of productive trees and the costs induced by fruit production and disease management [27].

In order to simulate wide range of epidemic and management scenarios, the model includes 6 epidemiological and 23 management parameters [27, 19]. In this work, we will use the 6 epidemiological parameters and only 10 management parameters to performed some optimizations quickly. Among the 23 management parameters, we removed parameters corresponding to plantation restrictions, removals, and surveillance of young orchards. The parameters we kept include distances of 3 zones for which the surveys are more or less frequent as well as their duration, the probability of the infected tree detection, and a contamination threshold which can request to increase the surveillance frequency in a focal zone. Details of management parameters used in this study are presented in Fig.1 and Table 1 (this table also includes the variation ranges of the parameters in the model).

Here, we aim to optimize the management strategy of the disease (i.e. to find the combination of management parameters allowing to obtain the best NPV), taking into account the epidemic stochasticity. However, we note that some combinations of management parameters can represent the same management, which may cause problems in the optimization process. Indeed, we observe that some management parameters are not useful when other parameters have a value of 0, which means that they can take any values without modifying the simulation. For example, when a zone radius is 0, the associated surveillance frequency have no impact on the NPV (regardless its value). The methodological developments that are proposed in this work address this issue by removing the parameter combinations which lead to the same management. The parameter invariances removed from the model are listed in Table 2.

Table 1 Management parameters implemented in the previously developed model with minimum and maximum values corresponding to the variation range of each parameter.

		Min	Max
ρ	Probability of detection of a symptomatic tree	0	0.66
γ_o	Duration of observation zones (year)	0	10
ζ_s	Radius of security zones (m)	0	5800
ζ_f	Radius of focal zones (m)	0	5800
ζ_{eo}	Radius of observation epicenter (m)	0	5800
$1/\eta_0$	Maximal period between 2 observations (year)	1	15
η_s	Observation frequency in security zones (year^{-1})	0	8
η_f	Observation frequency in focal zones (year^{-1})	0	8
η_{f*}	Modified observation frequency in focal zones (year^{-1})	0	8
χ_o	Contamination threshold in the observation epicenter, above which the observation frequency in focal zone is modified	0	1

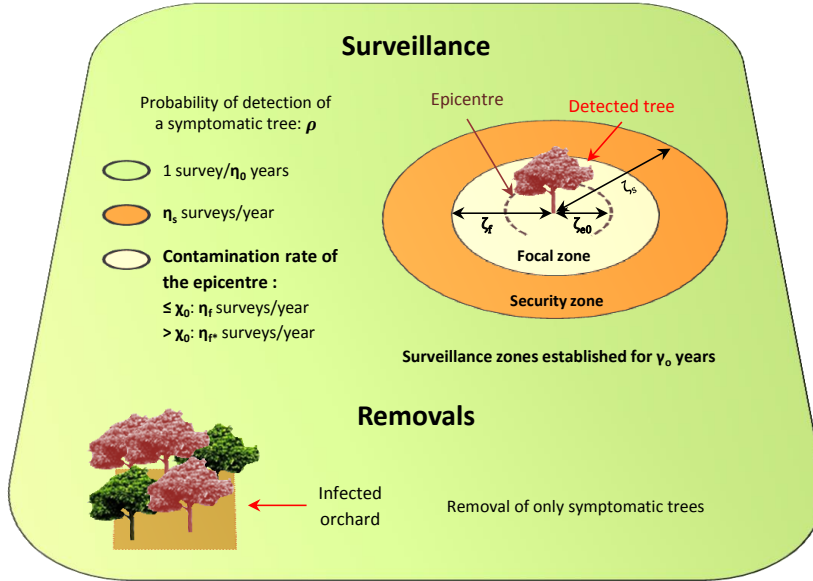


Fig. 1 Management actions implemented in the model.

3 Basics of Bayesian optimization

3.1 Gaussian process modeling

Bayesian optimization can be seen as a modernization of the statistical response surface methodology for sequential design [2], where the basic idea is to replace an

Table 2 Invariances of management parameters. For instance, when $\gamma_O = 0$ or when $\rho = 0$, χ_o does not influence the model output.

Management parameters	OR	OR	OR
χ_o	$\gamma_O = 0$	$\rho = 0$	
ζ_{eo}	$\gamma_O = 0$	$\zeta_s = 0$	$\rho = 0$
ζ_f	$\gamma_O = 0$	$\zeta_s = 0$	
η_{f*}	$\gamma_O = 0$	$\rho = 0$	
ζ_s	$\gamma_O = 0$	$\eta_s = 0$	
η_s	$\gamma_O = 0$		
η_f	$\gamma_O = 0$		

expensive-to-evaluate function by a cheap-to-evaluate surrogate one. In BO, Gaussian process (GP) regression, or kriging, is used to provide flexible response surface fits. GPs are attractive in particular for their tractability, since they are simply characterized by their mean $m(\cdot)$ and covariance (or kernel) $k(\cdot, \cdot)$ functions, see e.g., Rasmussen and Williams [24]. In the following, we consider zero-mean processes ($m = 0$) for the sake of conciseness.

Conditionally on n noisy observations $\mathbf{f} = (f_1, \dots, f_n)$, with independent, centered, Gaussian noise, that is, $f_i = y(\mathbf{x}_i) + \varepsilon_i$ with $\varepsilon_i \sim \mathcal{N}(0, \tau_i^2)$, the predictive distribution of y is another GP, with mean and covariance functions given by:

$$\mu(\mathbf{x}) = \mathbf{k}(\mathbf{x})^\top \mathbf{K}^{-1} \mathbf{f}, \quad (1)$$

$$\sigma^2(\mathbf{x}, \mathbf{x}') = k(\mathbf{x}, \mathbf{x}') - \mathbf{k}(\mathbf{x})^\top \mathbf{K}^{-1} \mathbf{k}(\mathbf{x}'), \quad (2)$$

where T denotes the tranposition operator, $\mathbf{k}(\mathbf{x}) := (k(\mathbf{x}, \mathbf{x}_1), \dots, k(\mathbf{x}, \mathbf{x}_n))^\top$ and $\mathbf{K} := (k(\mathbf{x}_i, \mathbf{x}_j) + \tau_i^2 \delta_{i=j})_{1 \leq i, j \leq n}$, δ standing for the Kronecker function.

Commonly, $k(\cdot, \cdot)$ belongs to a parametric family of covariance functions such as the Gaussian and Matérn kernels, based on hypotheses about the smoothness of y . Corresponding hyperparameters are often obtained as maximum likelihood estimates, see e.g., Rasmussen and Williams [24] or Roustant et al [29] for the corresponding details.

Note that in general, *stationary* covariances are used, i.e. k only depends on the distance $\|\mathbf{x} - \mathbf{x}'\|$ and not on the locations \mathbf{x} and \mathbf{x}' . This implies that the unconditional joint probability distribution of the process does not change when shifted in the \mathbb{X} space, which is in contradiction with the notion of local invariance.

3.2 Optimization

BO typically tackles optimization problems of the form:

$$\begin{aligned} \min \quad & y(\mathbf{x}) \\ \text{s.t. } & \mathbf{x} \in \mathbb{X}, \end{aligned}$$

with $\mathbb{X} \in \mathbb{R}^d$ is usually a bounded hyperrectangle and $y : \mathbb{R}^d \rightarrow \mathbb{R}$ is a scalar-valued objective function.

Optimization amounts here to choosing a sequence of points $\mathbf{x}_{n+1}, \dots, \mathbf{x}_{n+N}$ at which the function y is evaluated. Sequential design decisions, so-called *acquisitions*, are based on the GP model and judiciously balance exploration and exploitation in search for global optima. The GP model is updated after each new value is calculated.

In the noiseless setting ($\tau = 0$), the canonical acquisition function is *expected improvement* (EI) [13]. Define $f_{\min} = \min_{i=1,\dots,n} y_i$, the smallest y -value seen so far, and let $I(\mathbf{x}) = \max\{0, f_{\min} - Y(x)\}$ be the *improvement* at x . $I(x)$ is largest when $Y(\mathbf{x})$ has substantial distribution below f_{\min} . The expectation of $I(x)$ over $Y(x)$ has a convenient closed form, revealing balance between exploitation ($\mu(x)$ under f_{\min}) and exploration (large $\sigma^n(x)$):

$$\mathbb{E}\{I(x)\} = (f_{\min} - \mu(x))\Phi\left(\frac{f_{\min} - \mu(x)}{\sigma(x)}\right) + \sigma(x)\phi\left(\frac{f_{\min} - \mu(x)}{\sigma(x)}\right), \quad (3)$$

where $\Phi(\phi)$ is the standard normal cdf (and pdf respectively).

When y is only available through noisy evaluations, the EI acquisition cannot be used directly. Several authors have tackled this issue; we refer to [21] for a review on the topic. We chose here to focus on the *reinterpolation method* proposed in [11], which is based on the use of an instrumental noiseless kriging model, built from the original one. First, the (noisy) kriging predictions at the DOE points $\mu(\mathbf{x}_1), \dots, \mu(\mathbf{x}_n)$ are computed. Then, a reinterpolating model is built, by using the same covariance kernel and parameters and the same experimental design, but the observation vector is replaced by $\mu(\mathbf{x}_1), \dots, \mu(\mathbf{x}_n)$ and the noise variance is set to zero. Since this latter model is noise-free, the classical EI can be used as the infill criterion. Once the new design is chosen and the evaluation is performed, both kriging models are updated.

4 Bayesian optimization with invariances

4.1 Definition of local invariances

We first introduce the following notation (this is purely notation, no actual permutation is performed):

$$y(\mathbf{x}) = y(x_i, \mathbf{x}_J, \mathbf{x}_{-iJ}) \quad (4)$$

$$\mathbb{X} = \{\mathbb{X}_i, \mathbb{X}_J, \mathbb{X}_{-iJ}\} \quad (5)$$

Definition 1 (Simple) We call *simple invariance* the following case: y is invariant with respect to \mathbf{x}_J (J a subset of $\{1, \dots, d\} \setminus i$) if $x_i = c_i$ ($i \in \{1, \dots, d\}$):

$$y(c_i, \mathbf{x}_J, \mathbf{x}_{-iJ}) = y(c_i, \mathbf{x}'_J, \mathbf{x}_{-iJ}), \quad \forall \mathbf{x}_J, \mathbf{x}'_J \in \mathbb{X}_J, \mathbf{x}_{-iJ} \in \mathbb{X}_{-iJ}.$$

This corresponds for instance to the last line of Table 2: the observation frequency η_f does not have an effect on the model if the duration of observation γ_O is set to zero.

Definition 2 (Or) We call “*or*” *invariance* the following case: y is invariant with respect to \mathbf{x}_J (J a subset of $\{1, \dots, d\} \setminus I$) if there exists at least one $i \in I$ such that $x_i = c_i$ (I a subset of $\{1, \dots, d\} \setminus J$):

$$y(c_i, \mathbf{x}_{I \setminus i}, \mathbf{x}_J, \mathbf{x}_{-IJ}) = y(c_i, \mathbf{x}_{I \setminus i}, \mathbf{x}'_J, \mathbf{x}_{-IJ}), \quad \forall \mathbf{x}_J, \mathbf{x}'_J \in \mathbb{X}_J, \mathbf{x}_{I \setminus i} \in \mathbb{X}_{I \setminus i}.$$

This corresponds for instance to the first line of Table 2: the contamination threshold in the observation zone χ_o does not have an effect on the model if the duration of observation γ_O is set to zero or if the probability of detection ρ is set to zero.

Definition 3 (Linear) We call *linear invariance* the following case: y is invariant with respect to \mathbf{x}_J (J a subset of $\{1, \dots, d\} \setminus I$) if $\mathbf{A}\mathbf{x}_I = \mathbf{b}$, with I a subset of $\{1, \dots, d\} \setminus J$, \mathbf{A} a matrix of size $p \times \text{Card}(I)$ and \mathbf{b} a vector of size p :

$$y(\mathbf{x}_I, \mathbf{x}_J) = y(\mathbf{x}_I, \mathbf{x}'_J), \quad \forall \mathbf{x}_J, \mathbf{x}'_J \in \mathbb{X}_J, \text{ if } \mathbf{A}\mathbf{x}_I = \mathbf{b}.$$

There are two particular cases worth noting:

- setting $p = \text{Card}(I)$, $\mathbf{A} = \mathbb{I}_p$ and $\mathbf{b} = \mathbf{c}_I$ results in an “AND” condition: y is invariant with respect to \mathbf{x}_j if, $\forall i \in I, x_i = c_i$;
- setting $p = 1$, $\mathbf{A} = [1, -1]$ results in an invariance under the condition $x_{i1} = x_{i2}$.

This invariance case is not illustrated in this work with the sharka problem optimization presented here (with 10 management parameters). However, we may have this situation if we use all the parameters implemented in the model. For instance, a parameter γ_y (not used here) is implemented in the model. It corresponds to the duration of an observation zone for young orchards. In this case, the radius of observation epicenter ζ_{eo} does not have an effect on the model if the duration of observation zones γ_O is set to 0 AND if the duration of an observation zone for young orchards γ_y is also set to 0.

4.2 Principle of input warping

There are several ways of incorporating structural information into Gaussian processes. One is to work on the kernel function k [8, 6]. Another, which is the one we use here, is to transform the original input space \mathbb{X} into a *warped* one $\tilde{\mathbb{X}}$ and index the GP on $\tilde{\mathbb{X}}$, so that the new topology directly reflects the structural information [32, 15].

Consider for simplicity a single invariance over x_J when $x_i = c_i$. A simple way to handle this problem is to distort locally the space so that the subspace $\{(x_i, \mathbf{x}_J) | x_i = c_i\}$ collapses to a single point, for instance with \mathbf{x}_J at its average value: $(c_i, \overline{\mathbf{x}_J})$.

Hence, we are seeking warping functions of the form:

$$\begin{aligned} \psi : \mathbb{X} &\rightarrow \tilde{\mathbb{X}} \\ \mathbf{x} &\mapsto \tilde{\mathbf{x}} = \psi(\mathbf{x}) \end{aligned}$$

such that:

1. $\psi(x_i, \mathbf{x}_J, \mathbf{x}_{-iJ}) = (c_i, \overline{\mathbf{x}_J}, \mathbf{x}_{-iJ})$ if and only if $x_i = c_i$;
2. ψ restricted to $\mathbb{X} \setminus (c_i, ., .)$ and $\tilde{\mathbb{X}} \setminus (c_i, \overline{\mathbf{x}_J}, .)$ is a diffeomorphism.

In addition, we will search for deformations that decrease monotonically when $|x_i - c_i|$ increases, that is:

$$((x_i, \mathbf{x}_J, \mathbf{x}_{-iJ}), \psi[(x_i, \mathbf{x}_J, \mathbf{x}_{-iJ})]) \leq d((x'_i, \mathbf{x}_J, \mathbf{x}_{-iJ}), \psi[(x'_i, \mathbf{x}_J, \mathbf{x}_{-iJ})]) \\ \text{if } |x_i - c_i| \leq |x'_i - c_i|,$$

for some distance $d(., .)$.

Since the \mathbf{x}_J dimension collapses to $\overline{\mathbf{x}_J}$ at $x_i = c_i$, we write:

$$\forall j \in J, \quad \tilde{x}_j = \overline{x_j} + (x_j - \overline{x_j}) \alpha(x_i, c_i), \quad (6)$$

with $\alpha(x_i, c_i)$ an attenuation function such that:

1. $\alpha(c_i, c_i) = 0$;
2. α increases monotonically with $|x_i - c_i|$;
3. $0 < \alpha \leq 1, \forall x_i \neq c_i$.

Condition 1 ensures that $\widetilde{\mathbf{x}}_j = \overline{\mathbf{x}_J}$ when $x_i = c_i$ (all the dimensions in J collapse).

4.3 Warping for a simple invariance

In the simple invariance case, we propose linear and correlation-based attenuation functions:

$$\alpha_{\text{lin}}(x_i, c_i) = \frac{|x_i - c_i|}{\delta_i}, \quad (7)$$

$$\alpha_{\text{cor}}(x_i, c_i) = 1 - r(x_i, c_i), \quad (8)$$

where r is a $\mathbb{R} \times \mathbb{R} \rightarrow \mathbb{R}$ correlation function. Typically, δ_i may be set to the range of variation of x_i , so that the condition $\alpha \leq 1$ is ensured. Choosing r as the generalized exponential correlation, we have:

$$\alpha_{\text{exp}}(x_i, c_i) = 1 - \exp \left[- \left(\frac{|x_i - c_i|}{\theta_i} \right)^d \right], \quad (9)$$

with θ_i and d positive parameters to be tuned.

Figure 2 shows a 2D rectangular space distorted by three warpings, when the invariance is on a boundary of x_1 .

4.4 Warping for linear invariances

For simplicity, we consider first the particular linear case where $\mathbf{A} = \mathbb{I}_p$ and $\mathbf{b} = \mathbf{c}_I$, that is where invariances occur when a set of variables takes simultaneously a set of critical values: $\mathbf{Ax}_I = \mathbf{b}$, or equivalently $\mathbf{x}_I = \mathbf{c}_I$. In that case, a possible warping is:

$$\forall j \in J, \quad \tilde{x}_j = \overline{x_j} + (x_j - \overline{x_j}) \alpha_I(\mathbf{x}_I, \mathbf{c}_I). \quad (10)$$

with α_I now a multivariate attenuation function ($\mathbb{R}^{\text{Card}(I)} \times \mathbb{R}^{\text{Card}(I)} \rightarrow \mathbb{R}$), so that, similarly to the simple case:

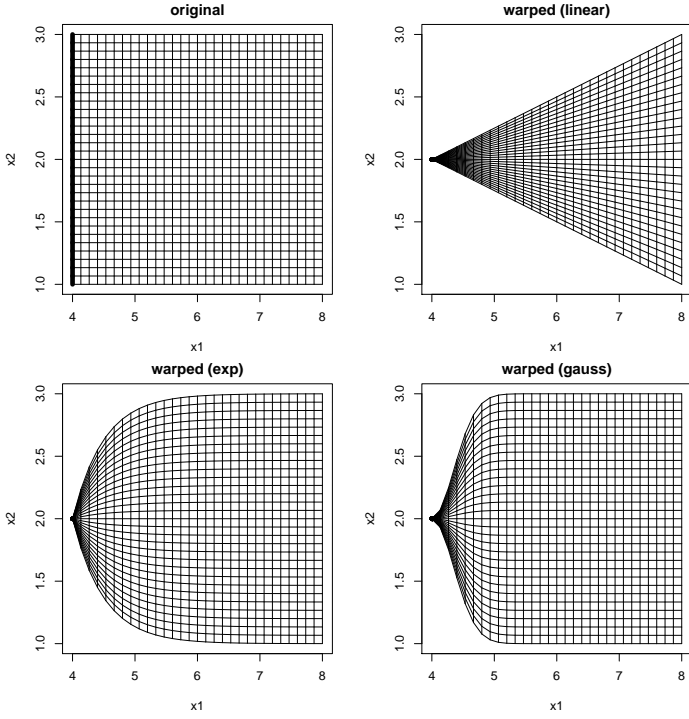


Fig. 2 Three deformations of a 2D space. The local invariance is at $x_1 = 0$, highlighted with larger lines.

1. $\alpha_I(\mathbf{c}_I, \mathbf{c}_I) = 0$;
2. α_I increases monotonically with $d(\mathbf{x}_I, \mathbf{c}_I)$ (for some distance $d(., .)$);
3. $0 < \alpha_I \leq 1, \forall \mathbf{x}_I \neq \mathbf{c}_I$.

As in the simple case, linear and correlation-based warpings can be defined as:

$$\alpha_{\text{lin}}(\mathbf{x}_I, \mathbf{c}_I) = \frac{1}{\text{Card}(I)} \sum_{i \in I} \frac{|x_i - c_i|}{\delta_i}, \quad (11)$$

$$\alpha_{\text{cor}}(\mathbf{x}_I, \mathbf{c}_I) = 1 - r_I(\mathbf{x}_I, \mathbf{c}_I), \quad (12)$$

with r_I a $\mathbb{R}^{\text{Card}(I)} \times \mathbb{R}^{\text{Card}(I)} \rightarrow \mathbb{R}$ correlation function as in 9.

Generalizing to the affine case $\mathbf{Ax}_I = \mathbf{b}$, the warping function is the same as in Equation 10, with now:

$$\alpha(\mathbf{x}_I, \mathbf{c}_I) = 1 - r_A(\mathbf{Ax}_I, \mathbf{b}). \quad (13)$$

4.5 Combining warpings

Independent conditions Now, we consider that we have a series of invariance conditions, defined with respect to sets I_1, \dots, I_n and corresponding J_1, \dots, J_n . If $J_k \cap J_l = \emptyset$, $1 \leq j \neq k \leq n$ and $I_i \cap J_k = \emptyset$, $1 \leq j, k \leq n$, the set of warped

variables are distinct from the set on which the conditions are written, the invariance conditions are written only once for each variable. In that case, the warpings can be applied independently.

Combinations of simple conditions: “OR” invariance Now, we consider the case when y is invariant w.r.t. a set \mathbf{x}_J for different conditions on sets I_1, \dots, I_n (that, for $\mathbf{x}_{I_1} = \mathbf{c}_{I_1}$ OR $\mathbf{x}_{I_2} = \mathbf{c}_{I_2}$ OR …). If $J \cap I_i = \emptyset$, $1 \leq i \leq n$, the warping function we propose is:

$$\forall j \in J, \quad \tilde{x}_j = \bar{x}_j + (x_j - \bar{x}_j) \prod_{I \in \{I_1, \dots, I_n\}} \alpha_I(\mathbf{x}_I, \mathbf{c}_I). \quad (14)$$

We see directly that the product of α 's ensure that $\tilde{x}_j = \bar{x}_j$ if any $x_i = c_i$, and the distortion reduces only when *all* the x_i 's are far from the c_i 's.

“Circular” conditions Difficulty only arises when some variables appear in both I_l 's and J_m 's sets. Take for instance a “reciprocal” condition, e.g., y is invariant w.r.t. \mathbf{x}_J when $\mathbf{x}_I = \mathbf{c}_I$, and invariant w.r.t. \mathbf{x}_I when $\mathbf{x}_J = \mathbf{c}_J$. In that case, applying independently warping functions would lead to:

$$\begin{aligned} \psi(\mathbf{c}_I, \mathbf{x}_J, \mathbf{x}_{-IJ}) &= (\mathbf{c}_I, \bar{\mathbf{x}}_J, \mathbf{x}_{-IJ}), \\ \psi(\mathbf{x}_I, \mathbf{c}_J, \mathbf{x}_{-IJ}) &= (\bar{\mathbf{x}}_I, \mathbf{c}_J, \mathbf{x}_{-IJ}), \\ \text{but: } \psi(\mathbf{c}_I, \mathbf{c}_J, \mathbf{x}_{-IJ}) &= (\mathbf{c}_I, \mathbf{c}_J, \mathbf{x}_{-IJ}), \end{aligned}$$

which induces a discontinuity.

In that case, a simple solution is to fix the non influent variable to its critical value instead of its average, hence applying:

$$\forall k \in K = (\cup_{1 \leq l \leq n} I_l) \cap (\cup_{1 \leq m \leq n} J_m), \quad \widetilde{x_k} = c_k + (x_k - c_k) \prod_{i \in I_k} \alpha(x_i, c_i) \quad (15)$$

Remark This formula does not apply in the affine case (Equation 13).

We show the deformations on a 2D space on Figure 3, where the two critical values are on the boundaries of x_1 and x_2 . Here, the warping of Equation 15 is applied on each variable ($K = \{1, 2\}$). Again, except for the linear warping, the local topology is preserved far from the critical edges.

4.6 Illustration

Finally, Figure 4 shows four deformations of the unit cubic space, for each of the following invariances:

- AND: y is invariant w.r.t. x_3 when x_1 AND x_2 are equal to zero (equation 10 with $I = 1$ and $J = \{1, 2\}$);
- OR: y is invariant w.r.t. x_3 when x_1 OR x_2 are equal to zero (equation 14 with $I = 1$ and $J = \{1, 2\}$);

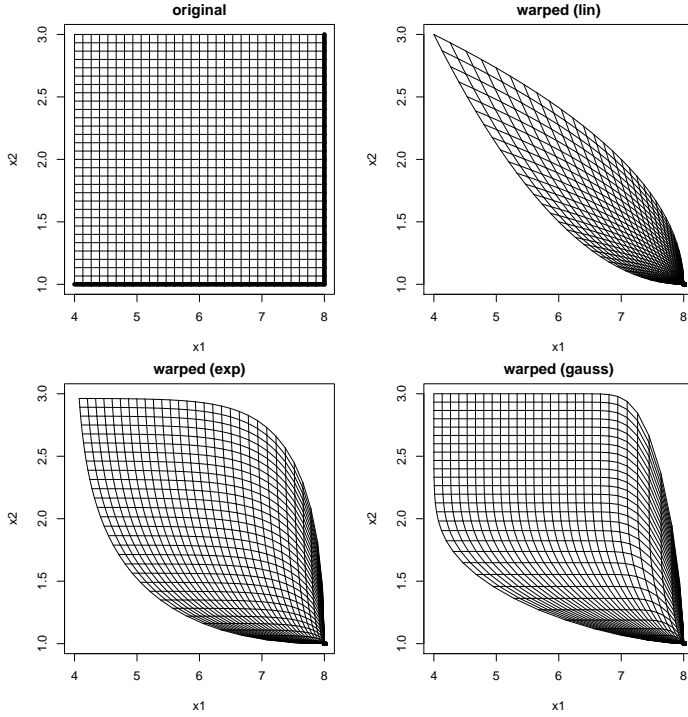


Fig. 3 Three deformations of a 2D space, with invariance at $x_1 = 8$ OR $x_2 = 1$, highlighted with larger lines.

- LINEAR: y is invariant w.r.t. x_3 when $x_1 = x_2 = 0$ (equation 13 with $I = 1$, $J = \{1, 2\}$, $\mathbf{A} = [1, -1]$ and $\mathbf{b} = 0$);
- CIRCULAR: y is invariant w.r.t. a- x_2 if $x_1 = 0$, b- x_3 if $x_2 = 0$, c- w.r.t. x_1 if $x_3 = 0$ (equation 15 with $K = \{1, 2, 3\}$, $C = [0, 0, 0]$ and $I_1 = 3$, $I_2 = 1$, and $I_3 = 2$).

On all cases, a Gaussian warping (exponential with $d = 2$) is applied, with range parameter $\theta = 0.3$.

4.7 Warping parameters tuning

The linear warping has the advantage of being parameter-free, which comes at a price of a profound modification of the problem topology. The correlation-based warpings have the capability of creating more localized distortions, but depend on range parameters (the θ_i 's in Equation 9). Those may be estimated by likelihood maximization along with the GP covariance parameters [32, 15].

However, we found in our numerical experiments that choosing the same correlation function for the GP and the warping, and fixing the warping ranges to be 1/10th of the GP ones provided very satisfactory results, while avoiding the extra computational burden.

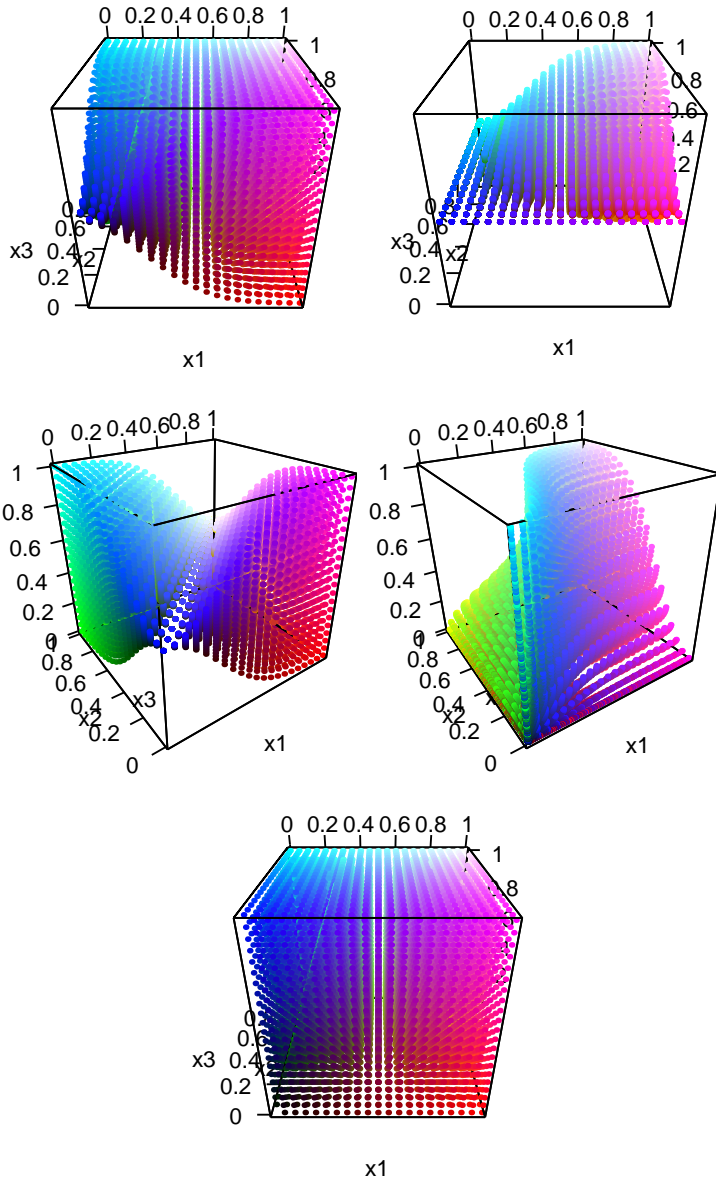


Fig. 4 Four deformations of the unit cube under different invariances: AND (top left), OR (top right), LINEAR (middle left), CIRCULAR (middle right). The bottom figure shows the orginal space.

Note that in the case of linear invariances, choosing the range of the correlation r_A is non-trivial, as it is not directly linked to design variables. A possible solution is $\theta_A = \mathbf{A}^T \boldsymbol{\theta}_I$.

4.8 Bayesian optimization on warped spaces

A decisive advantage of warping over alternative approaches is that it does not require any change of the BO apparatus. The GP modeling step is performed in the warped space $\tilde{\mathbb{X}}$ instead of the original one \mathbb{X} , that is, a standard GP model (i.e. stationary) is fitted to the transformed design of experiments $\{\tilde{\mathbf{x}}_1, y_1\}, \dots, \{\tilde{\mathbf{x}}_n, y_n\}$.

The acquisition maximization can be done directly in the original space:

$$\mathbf{x}_{n+1} \in \arg \max_{\mathbf{x} \in \mathbb{X}} EI[\psi(\mathbf{x})]. \quad (16)$$

Note that EI would exhibit the same invariances as the objective function.

Figure 5 shows unconditional realizations of GPs originally defined in the warped space but shown in the original space (using the inverse of the transformation ψ), for each of the warpings of Figure 2. We see that the invariance at $x_1 = 1$ is ensured. The linear warping induces a strong anisotropy, while with the two other warpings, the process seems stationary far from the critical value.

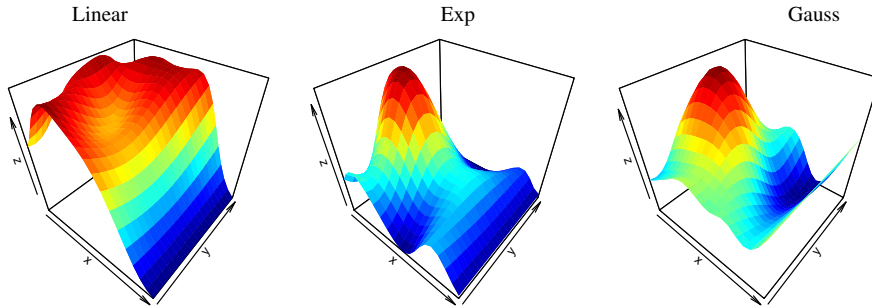


Fig. 5 Three GP realizations using warping functions as shown previously.

5 A warping-based Bayesian optimization of the Sharka model

5.1 Numerical setup

5.1.1 Experiments description

To assess the benefits of including the warping step in the optimization process (i.e. reducing the parameter space removing the combinations which lead to the same management), we conducted 50 independent optimizations of sharka management parameters with and without the warping step. Warping is applied to seven variables, following Table 2, to account for two simple invariances η_s, η_f , two combined ones χ_o, η_{f*} , and three implying “circular” conditions: ζ_{eo}, ζ_f and ζ_s . On all cases, we used a Matérn 5/2 correlation-based warping.

The economic criterion to optimize was the mean of the NPV (\overline{NPV}). For this to happen, we randomly selected 50 times 200 management strategies using a maximin

Latin hypercube sampling design [7]. Then, for each sampling design of 200 strategies, we performed 2 optimizations in parallel: with and without the warping step. For each optimization, we performed sequentially 200 iterations allowing to choose 200 new strategies, resulting in a total of 400 evaluated strategies. For each evaluated strategy, the objective function is computed by averaging over 1,000 simulations (carried out with different random seeds) to take into account the variability due to the epidemic and landscape characteristics.

5.1.2 Bayesian optimization setup

For all experiments, we used the same GP modeling setup, that is, an unknown constant trend (ordinary kriging, [16]) and Matérn 5/2 covariance function [24, Chapter 4]. The acquisition function maximized at each step is the expected improvement on the *reinterpolating* model. The maximization is performed by a large-scale random search followed by a local optimization starting for the optimum found by the random search (i.e. the evaluated points in the optimization process are chosen around the best current \overline{NPV}) All experiments were conducted in R [23], using code adapted from the DiceOptim package [20].

5.2 Results

We firstly compared the optimization results by subtracting the \overline{NPV} achieved using the optimization with the warping step and the optimization without the warping step (obtained from the same sampling design). In 24 out of the 50 optimization cases, we obtained better \overline{NPV} with the warping step than without. This point is illustrated by the probability density function which is centered on 0 (Fig.6). This result means that with 200 iterations in the optimization, the final optimization result is not impacted by the use of the warping.

However, we showed that the warping can impact the optimization speed (Fig.7). Indeed, at the 3rd iteration, the gap between the yellow (with warping) and the blue (without warping) lines is already 3957 euro/ha. In addition, to reach $\overline{NPV}=16,400$ euro/ha, we needed in average only 96 iterations in the optimization process with warping against 144 iterations without warping.

To go further, we performed a nonlinear regression of \overline{NPV} obtained for all the selected strategies during the optimization process with and without the warping step, and we compared the growth parameter c of the following regression: $\overline{NPV} = A + be^{-cx_i}$. This parameter was higher with (0.26) than without (0.18) warping.

In addition, we can visually observe that the warping step allow to improve the optimization speed on the Fig.8 and Supplementary Fig.1. These figures were represented with a specific algorithm based on empirical distribution functions [10]. Briefly, we uniformly defined 100 α values within a specified range. Then, for each iteration performed in the optimization process (i.e. for each of the 200 evaluated strategies), we add: the number of optimizations (among 50) which exceed α_1 , the number of optimizations which exceed α_2 , ..., the number of optimizations which exceed α_{100} . We used $\alpha \in [0;18,012.12]$ Supplementary (Fig.1) and $\alpha \in [10,000;18,012.12]$

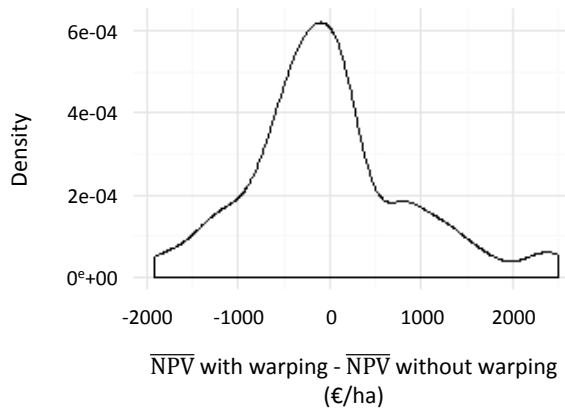


Fig. 6 Comparison of \overline{NPV} obtained at the end of the optimization with and without warping.

(Fig.8). The value 18,012.12 corresponds to the maximal value of \overline{NPV} identified in all the optimizations.

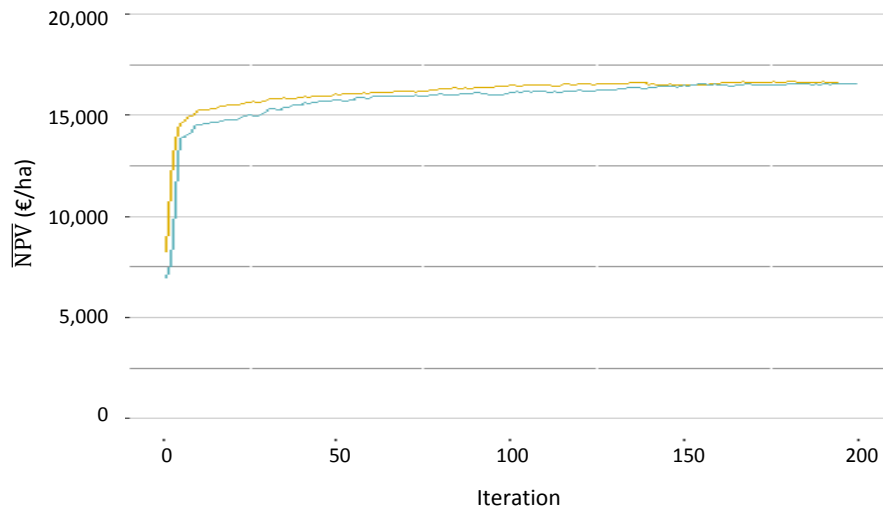


Fig. 7 Comparison of \overline{NPV} obtained during optimizations with and without warping. Yellow and blue lines represent the mean of the \overline{NPV} selected at each iteration for the 50 optimizations respectively performed with and without the warping step.

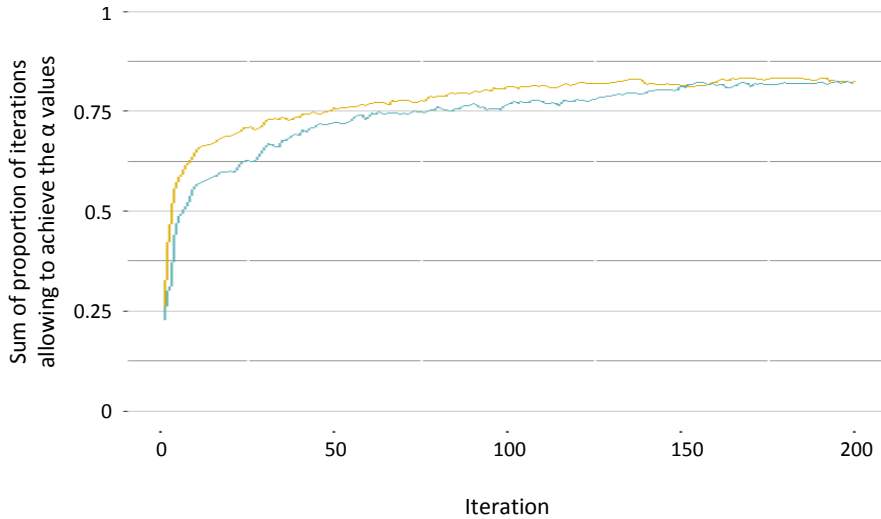


Fig. 8 Results of the algorithm using empirical distribution functions [10] with (yellow) and without (blue) warping ($\alpha \in [10,000;18,012.12]$).

6 Conclusion

In this study, we showed how a Bayesian optimization process can be improved by accounting for some prior structural information: the insensitivity of the model with respect to a subset of its input variables when another subset of inputs takes a particular value. Such *local invariances* were exhibited by our spatiotemporal model simulating shark management, characterized by 10 parameters related to the surveillance of the orchards. In this example, the invariances arise because parameters (radius of different zones, surveillance frequency in each zone, detection probability of infected trees, and duration of observation zones) are strongly related. Indeed, we easily note, for instance, that when the detection probability takes a value of 0, numerous other parameters do not influence the model results.

To tackle this problem, we proposed to use a warping of the input space, that here amounted to remove locally dimensions of the input space. The warping we used is based on correlation functions, making it very simple to implement while allowing sufficient flexibility. A particular advantage of input warping over other approaches is that it can be straightforwardly embedded in a BO algorithm.

We applied this Bayesian optimization process to the spatio-temporal sharka model. We performed various optimizations of its management parameters firstly with the use of warping (which allows accounting for the invariances) and then without. We showed that both approaches led to the same maximal \overline{NPV} , but the the optimization process with warping was substantially faster, showing that the warping efficiently reduced the search space without altering the exploration / exploitation trade-off.

As future steps for this research, we could first embed learning the warping parameters together with the parameters of the GP covariance in a single likelihood maximization step. Another room for improvement is to adapt the EI maximization

step to the new topology induced by the warping (here, on all experiments the EI was maximized over the original space). Finally, the optimization strategy pursued here used a large fixed number of replicates (1,000) for each evaluated design. Combining warping with an efficient adaptative scheme to handle replicates [12] would drastically reduce the cost of the optimization.

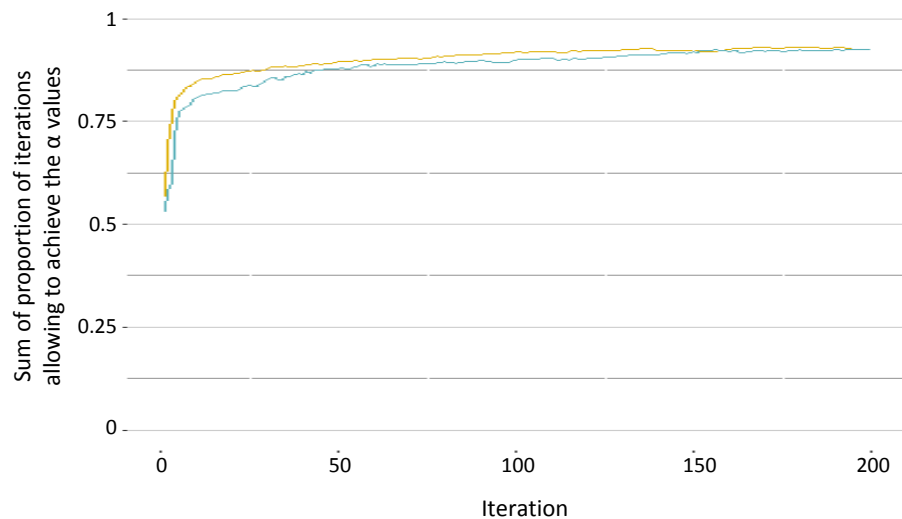
References

1. Bajardi P, Barrat A, Savini L, Colizza V (2012) Optimizing surveillance for live-stock disease spreading through animal movements. *Journal of the Royal Society Interface* 9(76):2814–2825
2. Box GE, Draper NR (1987) Empirical model-building and response surfaces. John Wiley & Sons
3. Cambra M, Capote N, Myrta A, Llácer G (2006) Plum pox virus and the estimated costs associated with sharka disease. *EPPO Bulletin* 36(2):202–204
4. Cunniffe NJ, Koskella B, Metcalf CJ, Parnell S, Gottwald TR, Gilligan CA (2015) Thirteen challenges in modelling plant diseases. *Epidemics* 10:6–10
5. Cunniffe NJ, Cobb RC, Meentemeyer RK, Rizzo DM, Gilligan CA (2016) Modeling when, where, and how to manage a forest epidemic, motivated by sudden oak death in California. *Proceedings of the National Academy of Sciences of the United States of America* 113(20):5640–5645
6. Duvenaud D (2014) Automatic model construction with gaussian processes. PhD thesis, University of Cambridge
7. Fang KT, Li R, Sudjianto A (2005) Design and modeling for computer experiments. Chapman and Hall/CRC
8. Ginsbourger D, Durrande N, Roustant O (2013) Kernels and designs for modelling invariant functions: From group invariance to additivity. In: mODa 10—Advances in Model-Oriented Design and Analysis, Springer, pp 107–115
9. Grechi I, Ould-Sidi MM, Hilgert N, Senoussi R, Sauphanor B, Lescourret F (2012) Designing integrated management scenarios using simulation-based and multi-objective optimization: Application to the peach tree–myzus persicae aphid system. *Ecological Modelling* 246:47–59
10. Hansen N, Auger A, Ros R, Finck S, P P (2010) Comparing results of 31 algorithms from the black-box optimization benchmarking bbob-2009. *Proceedings of the 12th annual conference companion on Genetic and evolutionary computation* pp 1689–1696
11. J Forrester AJ, Keane AJ, Bressloff NW (2006) Design and analysis of “noisy” computer experiments. *AIAA journal* 44(10):2331–2339
12. Jalali H, Van Nieuwenhuyse I, Picheny V (2017) Comparison of kriging-based algorithms for simulation optimization with heterogeneous noise. *European Journal of Operational Research* 261(1):279–301
13. Jones DR, Schonlau M, Welch WJ (1998) Efficient global optimization of expensive black-box functions. *Journal of Global Optimization* 13(4):455–492
14. Kompas T, Ha PV, Nguyen HTM, East I, Roche S, Garner G (2017) Optimal surveillance against foot-and-mouth disease: the case of bulk milk testing in aus-

- tralia. *Australian Journal of Agricultural and Resource Economics* 61(4):515–538
15. Marmin S, Ginsbourger D, Baccou J, Liandrat J (2018) Warped gaussian processes and derivative-based sequential designs for functions with heterogeneous variations. *SIAM/ASA Journal on Uncertainty Quantification* 6(3):991–1018
 16. Matheron G (1963) Principles of geostatistics. *Economic Geology* 58(8):1246–1266
 17. Mockus J (2012) Bayesian approach to global optimization: theory and applications, vol 37. Springer Science & Business Media
 18. Mushayabasa S, Tapedzesa G (2015) Modeling the effects of multiple intervention strategies on controlling foot-and-mouth disease. *BioMed research international*
 19. Picard C, Soubeyrand S, Jacquot E, Thébaud G (2018) Analyzing the influence of landscape aggregation on disease spread to improve management strategies. (under review)
 20. Picheny V, Ginsbourger D (2014) Noisy kriging-based optimization methods: a unified implementation within the DiceOptim package. *Computational Statistics & Data Analysis* 71:1035–1053
 21. Picheny V, Wagner T, Ginsbourger D (2013) A benchmark of kriging-based infill criteria for noisy optimization. *Structural and Multidisciplinary Optimization* 48(3):607–626
 22. Pleydell DRJ, Soubeyrand S, Dallot S, Labonne G, Chadoeuf J, Jacquot E, Thébaud G (2018) Estimation of the dispersal distances of an aphid-borne virus in a patchy landscape. *PLoS Computational Biology* 14(4):e1006085
 23. R Core Team (2018) R: A Language and Environment for Statistical Computing. R Foundation for Statistical Computing, Vienna, Austria, URL <https://www.R-project.org/>
 24. Rasmussen CE, Williams C (2006) Gaussian Processes for Machine Learning. MIT Press, URL <http://www.gaussianprocess.org/gpml/>
 25. Rimbaud L, Dallot S, Gottwald T, Decroocq V, Jacquot E, Soubeyrand S, Thébaud G (2015) Sharka epidemiology and worldwide management strategies: learning lessons to optimize disease control in perennial plants. *Annual Review of Phytopathology* 53:357–378
 26. Rimbaud L, Bruchou C, Dallot S, Pleydell DRJ, Jacquot E, Soubeyrand S, Thébaud G (2018) Using sensitivity analysis to identify key factors for the propagation of a plant epidemic. *Royal Society Open Science* 5(1):171435
 27. Rimbaud L, Dallot S, Bruchou C, Thoyer S, Jacquot E, Soubeyrand S, Thébaud G (2018) Heuristic optimisation of the management strategy of a plant epidemic using sequential sensitivity analyses. *BioRxiv* 315747
 28. Rios LM, Sahinidis NV (2013) Derivative-free optimization: a review of algorithms and comparison of software implementations. *Journal of Global Optimization* 56(3):1247–1293
 29. Roustant O, Ginsbourger D, Deville Y (2012) DiceKriging, DiceOptim: Two R packages for the analysis of computer experiments by kriging-based metamodeling and optimization. *Journal of Statistical Software* 51(1):1–55, URL <http://www.jstatsoft.org/v51/i01/>

30. Shahriari B, Swersky K, Wang Z, Adams RP, De Freitas N (2016) Taking the human out of the loop: A review of bayesian optimization. *Proceedings of the IEEE* 104(1):148–175
31. Snelson E, Ghahramani Z, Rasmussen CE (2004) Warped gaussian processes. In: *Advances in neural information processing systems*, pp 337–344
32. Snoek J, Swersky K, Zemel R, Adams R (2014) Input warping for bayesian optimization of non-stationary functions. In: *International Conference on Machine Learning*, pp 1674–1682
33. Tildesley MJ, Savill NJ, Shaw DJ, Deardon R, Brooks SP, Woolhouse ME, Grenfell BT, Keeling MJ (2006) Optimal reactive vaccination strategies for a foot-and-mouth outbreak in the UK. *Nature* 440(7080):83
34. VanderWaal K, Enns EA, Picasso C, Alvarez J, Perez A, Fernandez F, Gil A, Craft M, Wells S (2017) Optimal surveillance strategies for bovine tuberculosis in a low-prevalence country. *Scientific Reports* 7(1):4140

Supporting information



Supplementary Figure 1 Results of the algorithm using empirical distribution functions [10] with (yellow) and without (blue) warping ($\alpha \in [0;18,012,12]$).